Volume 1 | Number 1 | Jan 2013 | Pages 1–100

PCCP

Physical Chemistry Chemical Physics
www.rsc.org/pccp

ROYAL SOCIETY OF CHEMISTRY

ROYAL SOCIETY OF CHEMISTRY

www.rsc.org/pccp

The application of inelastic neutron scattering to investigate the interaction of methyl propanoate with silica

Andrew R McFarlane,[a] Hannah Geller,[a] Ian P. Silverwood,[a] Richard I. Cooper,[b] David J. Watkin,[b] Stewart F. Parker,[b] John M. Winfield[a] and David Lennon[*a]

[a]   School of Chemistry, Joseph Black Building, University of Glasgow, Glasgow, G12 8QQ, UK.
        E-mail: David.Lennon@glasgow.ac.uk
[b]   Chemical Crystallography, Chemistry Research Laboratory, Mansfield Road, Oxford OX1 3TA, UK
[c]   ISIS Facility, STFC Rutherford Appleton Laboratory, Chilton, Didcot, Oxon OX11 0QX, UK.

2

Abstract

A modern industrial route for the manufacture of methyl methacrylate involves the reaction of methyl propanoate and formaldehyde over a silica-supported Cs catalyst. Although the process has been successfully commercialised, little is known about the surface interactions responsible for the forward chemistry. This work concentrates upon the interaction of methyl propanoate over a representative silica. A combination of infrared spectroscopy, inelastic neutron scattering, DFT calculations, X-ray diffraction and temperature-programmed desorption is used to deduce how the ester interacts with the silica surface.

Keywords: methyl propanoate; silica; adsorption; inelastic neutron scattering, infrared spectroscopy.

1.   Introduction

The synthesis of acrylic compounds represents a major component of the modern chemical manufacturing sector. The products of this industry include furniture, automobile components, mobile phone screens and high definition LCD panels for use in TV and computer screens. Methyl methacrylate ($CH_2C=C(CH_3)-C(=O)-OCH_3$, MMA) is the essential ingredient for all these materials and has a global demand in excess of 2.2 million tonnes.[1] In 2005 there were over 30 manufacturing plants worldwide,[2] demonstrating the economic significance of chemistry related to the synthesis of methyl methacrylate. Many companies have been involved in developing the synthesis of MMA and over 17 possible synthetic routes are reported.[1]

The conventional route to MMA is the acetocyanohydrin (ACH) process. This reaction produces HCN from CH_4 and NH_3, which is then reacted with acetone to form ultimately MMA. However, throughout the world, new routes using a variety of reagents are currently being developed.[1,3] One of the main drivers for this development is the avoidance of manufacturing, storing and transporting the highly toxic hydrogen cyanide; the risk potential for this chemical is dependent on the specific process operation. Another problem with the ACH reaction is the formation of bisulfate by-products, which reduce the atom economy of the overall process. Lucite International, a global leader in the design, development and manufacture of acrylic-based products,[4] has developed the Alpha process [2,4] (see Scheme 1) which, in addition to representing dramatic improvements in operational performance, makes uses of readily available raw materials (ethene, methanol, and carbon monoxide) and combines a homogeneous catalytic stage followed by a heterogeneous catalytic stage to produce MMA in a more efficient and sustainable manner.[2] Such innovation in the chemical manufacturing industry has the potential to revolutionise operational practices. As part of that process, there needs to be an increasing awareness of the chemical interactions that favour the chemical transformations under consideration.
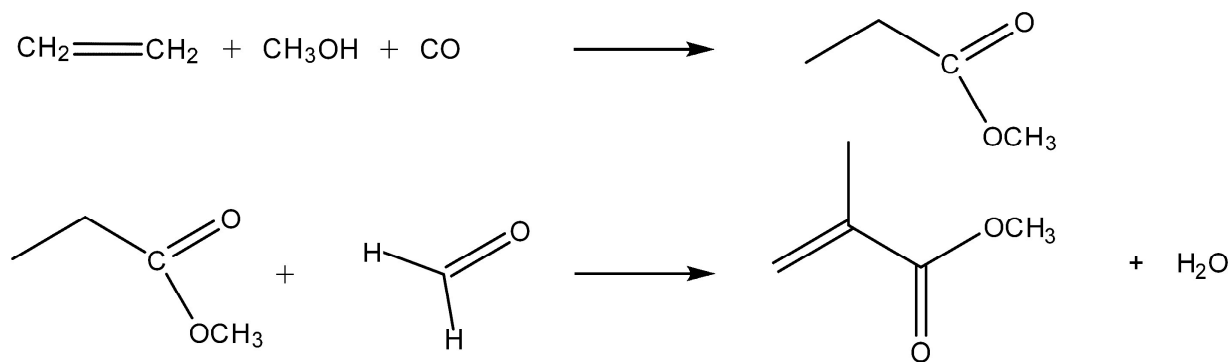
Scheme 1: The Alpha Process; the manufacture of methyl methacrylate from ethene, methanol and CO *via* methyl propanoate.[2,4,5]

An important part of the Alpha Process involves a reaction between methyl propanoate ($CH_3COOCH_2CH_3$), and formaldehyde (H_2CO); special handling procedures are required for the large scale use and storage of formaldehyde. Typically this heterogeneously catalysed reaction takes place over a modified silica catalyst, *e.g.* caesium nitrate supported on high surface area silica.[5] The reaction is thought to be an example of base catalysis, with the catalyst presenting basic sites that control the chemisorption and subsequent reaction of the two reagents. However, a survey of the literature indicates a paucity of work examining the interaction of oxygenates and esters in particular on oxide surfaces. Preliminary studies on silicas similar to that used with the Alpha process are believed to indicate the presence of both weak Brønsted acid and Brønsted base sites,[2] although the evidence for these assertions is not in the public domain.

This paper is divided into two parts. To our knowledge, methyl propanoate has been neither structurally nor spectroscopically characterised; thus, Part 1 provides a comprehensive description of the solid state structure and vibrational spectroscopy of methyl propanoate in the gas, liquid and solid phases, with assignments supported by periodic density functional theory (DFT). In Part 2 we characterise the adsorption of methyl propanoate on a representative silica (Fuji Q-10 silica spheres). Previous work by Jackson and co-workers examined the adsorption of acetic acid on this particular silica, as well as Cs-doped Q-10, with the latter constituting model methyl methacrylate synthesis catalysts.[6] That work followed on from a patent filed in 1999 by Jackson and co-workers at ICI (UK) entitled 'novel catalyst for manufacture of ethylenically unsaturated acids or esters, especially for manufacture of methyl methacrylate'.[7] Silica spheres, as opposed to silica powder, are attractive to industrial use as bulk handling properties are simplified. Against this background, Fuji Q-10 silica is examined in this communication. The combined structural and spectroscopic investigations establish the adsorption geometry for methyl propanoate adsorbed on this silica. The work is not extended to consider Cs-doped silica samples.

2.   Experimental section

2.1   X-ray crystallography

A sample of methyl propanoate (Aldrich, 99%, used as received) was sealed in a 0.5 mm Lindeman tube and flash-frozen in liquid nitrogen to confirm that the material did not form a glass. The sample was then mounted on a goniometer head with both arcs and translational adjustment so that the tube could be made co-linear with the diffractometer phi axis. The Enraf–Nonius KCCD diffractometer was set to $\theta = 20°$, $\omega = 180°$, $\chi = 90°$ and Dx =165 so that the ϕ axis was horizontal and perpendicular to the X-ray beam, and the locally constructed computer-controlled sample heating element installed.

The sample was chilled to a polycrystalline mass at 150 K using an Oxford Cryosystems Series 600 Cryostream.[8] The sample was zone-refined until it looked clear, but a short φ rotation image indicated that the sample still contained several large crystals lying parallel to the Lindeman tube axis. Further zone refinement failed to produce a single-crystal.

A new sample was prepared in a 0.1 mm Lindeman tube. This also produced aligned poly-crystals, but prolonged zone refinement converted the sample to a major component and several minor components. This size differentiation enabled diffraction images collected at κ=60° (to offset the tube axis from the scan axis) to be indexed. All three cell angles were quite close to 90°. A triclinic data set was collected in $P\bar{1}$ using four different scan regions. Because of the possibility that the cell was really monoclinic, reflections from each scan region were indexed independently. All gave essentially the same triclinic cell. The whole data set was then processed using the initial indexing, and the cell parameters refined from all of the data.

The H atoms were all located in a difference map, but those attached to carbon atoms were repositioned geometrically. The H atoms were initially refined with soft restraints on the bond lengths and angles to regularize their geometry (C—H in the range 0.93–0.98 Å) and $U_{iso}(H)$ (in the range 1.2–1.5 times U_{eq} of the parent atom), after which the positions were refined freely.

Data collection: *COLLECT* [9].; data reduction and cell refinement: *DENZO/SCALEPACK* [10]; programme used to solve structure: Superflip [11]; programme used to refine structure: *CRYSTALS* [12]; molecular graphics: CAMERON [13]. The data has been deposited with the Cambridge Structural Database (CSD) with deposition number: CCDC 1453909.

2.2 Computational methods

Periodic density functional theory (periodic-DFT) calculations of the crystal structure were carried out using the plane-wave pseudopotential method implemented in the CASTEP code.[14,15] Exchange and correlation were approximated using the PBE functional. Norm-conserving pseudopotentials with a plane-wave cut-off energy of 830 eV were used. Brillouin-zone sampling of electronic states was performed on a 4×4×2 Monkhorst-Pack grid. The equilibrium structure, an essential prerequisite for lattice dynamics calculations was obtained by BFGS geometry optimization, after which the residual forces were converged to zero within $|0.0008|$ eV Å^{-1}. Phonon frequencies were obtained by diagonalisation of dynamical matrices computed using density functional perturbation theory (DFPT).[15] An analysis of the resulting eigenvectors was used to map the computed modes to the corresponding irreducible representations of the point group and assign IUPAC symmetry labels. DFPT was also used to compute the dielectric response and the Born effective

charges and from these the mode oscillator strength tensor and infrared absorptivity were calculated. Conformational analysis of the isolated molecule was carried out with Gaussian 03.[16] The B3LYP functional with the 6-311g(d) basis set was used to generate a 2D relaxed potential energy scan about the central C2–C3 and the C3–O2 bonds (see Fig. 1 for the numbering scheme). To model methyl propanoate on silica, the B3LYP functional with the 6-31g basis set was used. INS spectra were generated from the output of CASTEP and Gaussian with ACLIMAX.[17] We emphasise that the transition energies determined by either CASTEP or Gaussian have *not* been scaled.
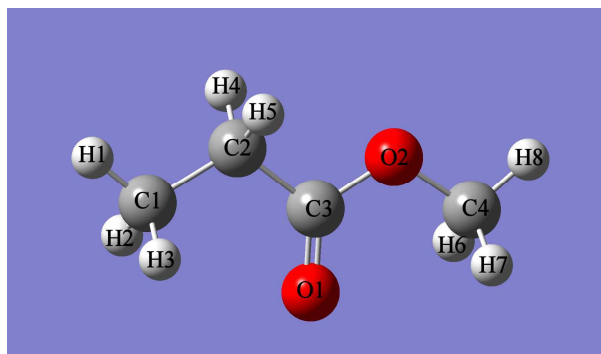

Fig. 1 Numbering scheme for methyl propanoate.

2.3   Temperature-programmed desorption and infrared spectroscopy

The silica used in all experiments was provided by Fuji (Cariact Q10). As received spheres of 2-3 mm diameter exhibited a surface area of 359 m^2 g^{-1} ,a pore volume of 1.01 cm^3 g^{-1} and a hydroxyl group density of 2.12 mmol g^{-1}.[6] Samples were prepared by grinding the silica into particles of size fraction 250-500 μm. Adsorption measurements were performed using a facility described elsewhere.[18] Briefly, silica samples were loaded in to a ¼" od stainless steel tubular reactor. Methyl propanoate (Aldrich, 99 % purity) was contained in a bubbler arrangement in advance of the reactor so that methyl propanoate vapour could be exposed to the catalyst in a controlled manner. Prior to adsorption measurements, activation of the silica was carried out by heating the silica under flowing helium (10 ml min^{-1}) for one hour at 623 K.[6] Post-activation, the sample was allowed to cool to 353 K and maintained at this temperature during exposure to a vapour stream of methyl propanoate. After a defined exposure period, the methyl propanoate flow was terminated whilst maintaining the helium flow for 30 min at 353 K. Thereafter, the sample was allowed to cool to 303 K in a continuous stream of helium. These arrangements disfavoured formation of physisorbed ester.

A quadrupole mass spectrometer (MKS Microvision Plus) was mounted downstream of the reactor, sampling the eluting gases *via* a differentially pumped capillary line and a sintered metal filter. Temperature-programmed desorption measurements were performed at a heating rate of 12 K min^{-1} up to 653 K whilst the mass spectrometer monitored the methyl propanoate signal intensity. *In situ* infrared spectroscopy of methyl propanoate adsorption was performed using a diffuse reflectance Smart Collector (Spectra-Tech) environmental cell housed inside a Nicolet Nexus FTIR spectrometer. Silica activation and methyl propanoate exposure were performed in the same manner as that employed for the tubular reactor. Spectra presented are background subtracted, using a spectrum of the activated silica as a background.

Transmission infrared spectroscopic measurements of methyl propanoate as a gas, liquid and solid utilised the same FTIR instrument but respectively coupled to the following sample cells: a Graseby-Specac 5660 heated gas cell, a Specac GS01800 liquid cell and a Specac GS21252 variable temperature cell.

2.4 Inelastic neutron scattering spectroscopy

Inelastic neutron scattering (INS) spectroscopy is a complementary form of vibrational spectroscopy that emphasises hydrogen motion.[19] This has the consequence that silica is essentially transparent to neutrons and the entire 0 – 4000 cm^{-1} range is accessible, in particular there is no spectral cut-off at ~1400 cm^{-1} as there is for infrared spectroscopy. INS spectra were recorded using the MAPS [20] and TOSCA [21] spectrometers at ISIS.[22] On TOSCA the resolution is ~ 1.25% of the energy transfer across the entire energy range, while on MAPS, under the conditions used here, it is ~1.5% of the incident energy at the largest energy transfer and degrades with decreasing energy transfer. Thus TOSCA provides excellent energy resolution at energy transfers <1600 cm^{-1}, at larger energy transfer MAPS provides better resolution by virtue of the access to low momentum transfer.[20] TOSCA and MAPS are highly complementary and enable the complete range of interest, 0 – 4000 cm^{-1}, to be covered with reasonable resolution.

For the INS experiments, silica (Fuji Q10 silica spheres) was dried using a previously described gas manifold [23] in a flow-through Inconel™ cell under flowing helium at 623 K for 90 mins and left to cool overnight. This sample was then measured as a background. A second sample was similarly dried, allowed to cool to 353 K and methyl propanoate introduced as a vapour stream entrained in helium gas *via* a Dreschel bottle. The INS spectra of the samples were then recorded.

3. Results and Discussion

Part 1: Characterisation of methyl propanoate

The structure of methyl propanoate as determined by a single crystal X-ray diffraction study is shown in Fig. 2. The crystal is triclinic, space group $P\bar{1}$ with $Z' = 2$ ($Z= 4$) (see Table S1 for the crystal data). One of the independent molecules is almost planar with C_s symmetry, the other has a torsion angle of 159.7º about the central C2–C3 bond and C_1 symmetry. There is no evidence of disorder or pseudo-symmetry. A periodic-DFT calculation (CASTEP) of the structure using the crystal structure as the initial input gives results in good agreement with the observed structure. A comparison of selected structural parameters is given in Table S2.
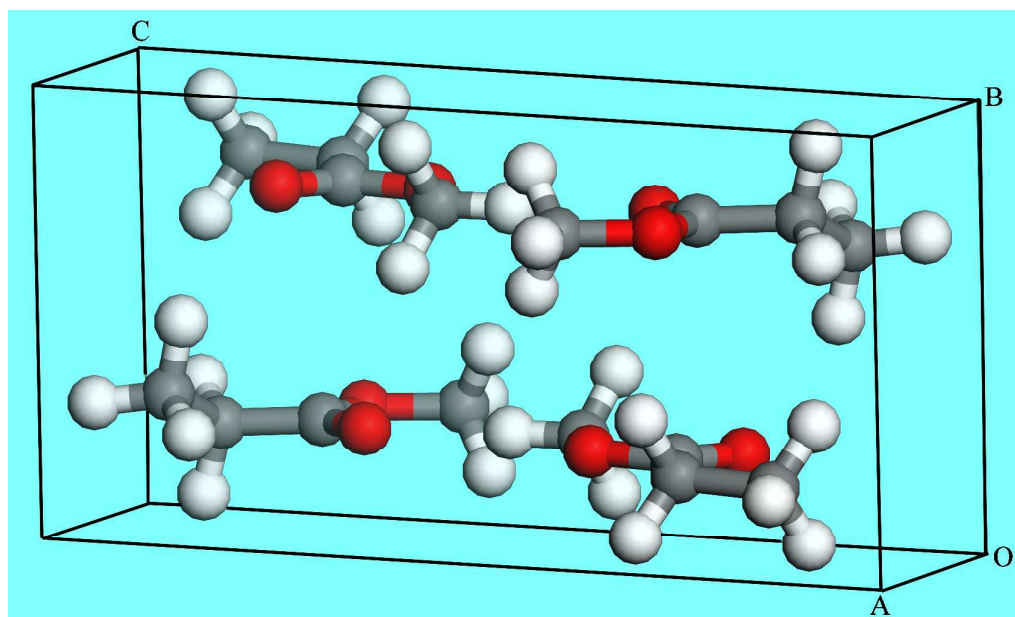

Fig. 2 $P\bar{1}$ crystal structure of methyl propanoate at 150 K. The molecules at the bottom right and top left have approximate C_s symmetry and those at the bottom left and top right have C_1 symmetry.

The conformational isomerism was also investigated with Gaussian 03 by starting from the planar C_s structure and carrying out a relaxed potential energy scan about the central C2–C3 bond and also about the C–OCH₃ (C3–O2) bond. The results are shown in Fig. 3. It can be seen that the planar C_s conformation is the lower energy structure. The C_1 conformation found in the solid state is ~5 kJ mole^{-1} higher in energy.
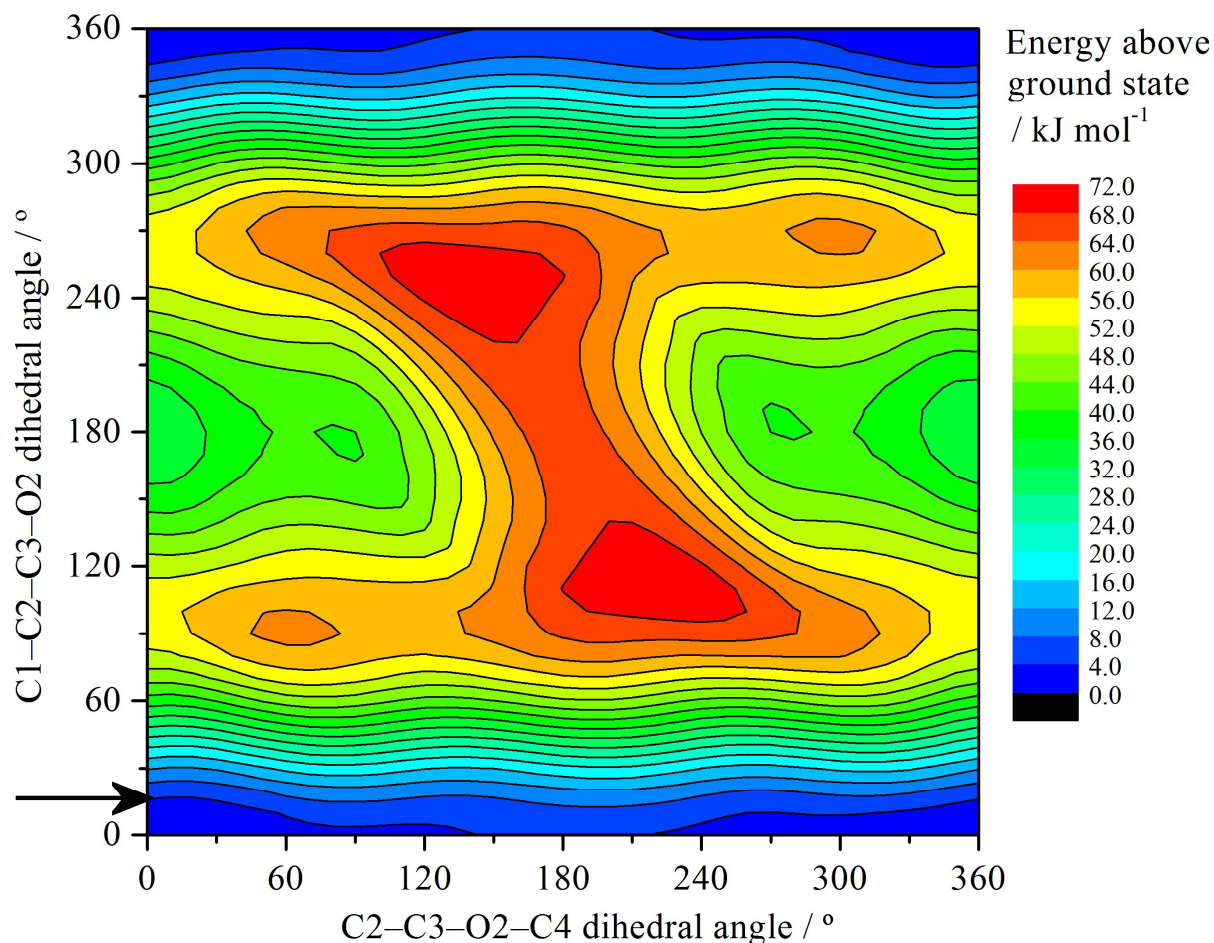
Fig. 3 2D potential energy scan of methyl propanoate. The four corners correspond to methyl propanoate with C_s symmetry, the arrow indicates the structure of the molecule with C_1 symmetry.

The infrared spectra of the gas, liquid and solid are shown in Fig. 4a-c and the inelastic neutron scattering (INS) spectrum of the solid is presented in Fig. 5a. Calculation of the spectra using the energy minimised structure finds all real transition energies, confirming that this is a stable structure. The calculated infrared and INS spectra of the solid are also shown in Figs. 4d and 5b. It can be seen that while the peaks are shifted lower energy, generally the relative intensities of the modes are well-reproduced. (The discrepancy in energy is apparent because we do not scale the spectra). Note that the calculated infrared spectrum assumes a constant linewidth; this is not correct for the C–O and C=O stretch modes at 1160 and 1700 cm^{-1} (they are broadened by the hydrogen bonding). The agreement in the C–H stretch region is poorer because these modes are strongly affected by anharmonicity that is not included in our model. In the low energy region, the discrepancy in the calculated positions is emphasised by the large x-scale used. In Fig. 5b, the pattern in the range 100 – 300 cm^{-1} is repeated by the calculated spectrum. Below 100 cm^{-1} the acoustic modes occur, these are seen in the INS spectrum but are not present in the calculation because it is a Γ-point

only calculation where the acoustic modes have zero energy. To reproduce these would require an expensive full dispersion calculation, which we could not justify for what would be a relatively minor improvement. Table 1 lists modes that are of relevance to the investigation of the adsorbed species described in Part 2; a complete assignment is given in Table S3.
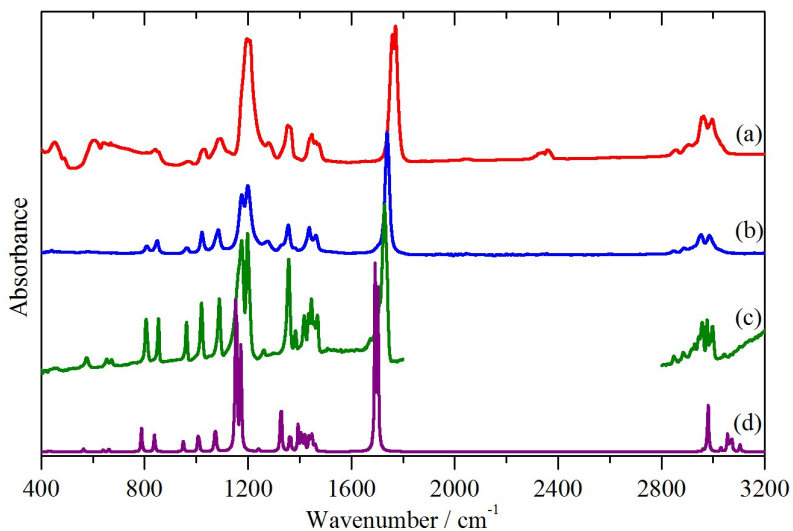
Table 1 hereabouts

Fig. 4 Infrared spectra of methyl propanoate: (a) gas, (b) liquid (both at room temperature), (c) solid at 130 K and (d) CASTEP calculated solid state spectrum.
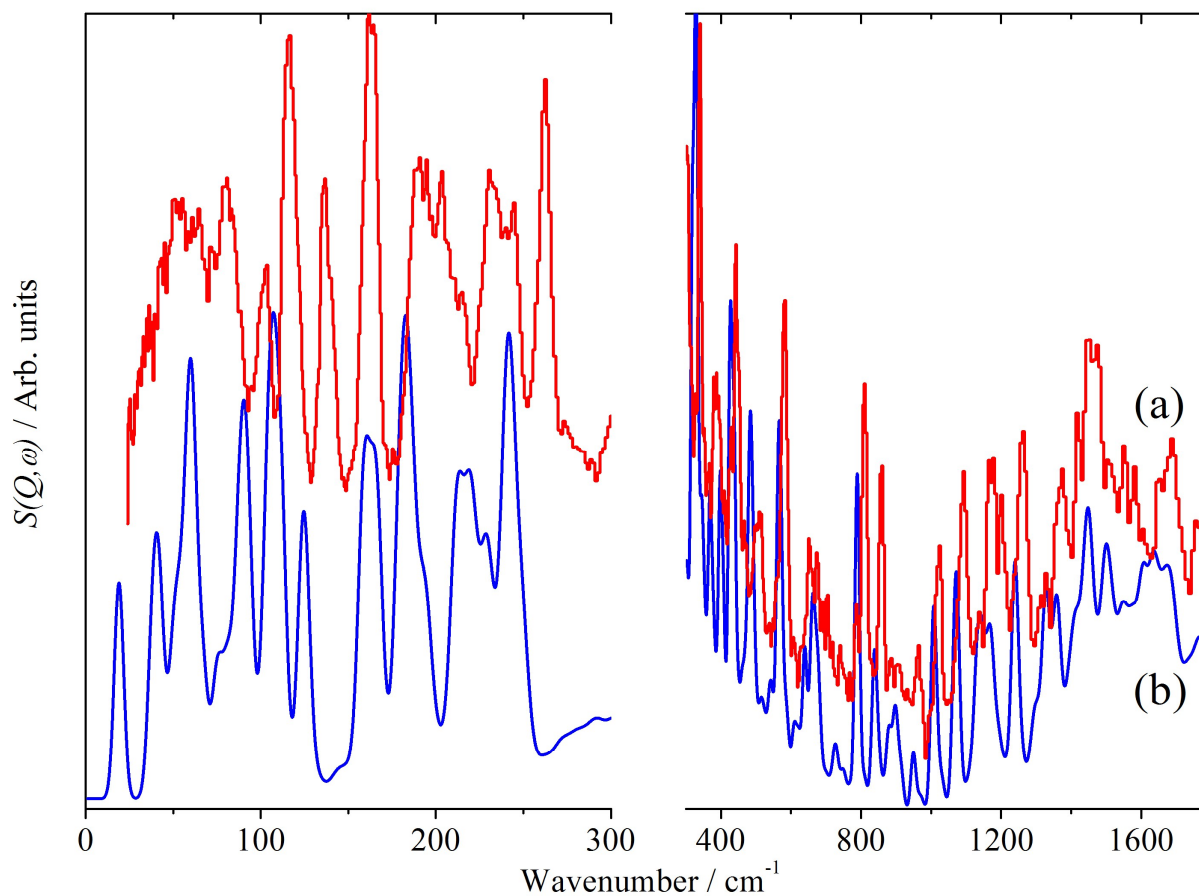
Fig. 5 INS spectra of: (a) solid methyl propanoate at 20 K and (b) CASTEP calculated solid state spectrum. The range 300 – 1800 cm^{-1} is ordinate expanded ×4 relative to the 0 – 300 cm^{-1} region.

Part 2: The adsorption of methyl propanoate on silica

Methyl propanoate was adsorbed on silica (activated by drying at 623 K) at 353 K (to minimise physisorption) then purged at 303 K for two hours. The sample was then heated to 673 K in 50 K steps, cooled to 303 K after each step and the infrared spectrum recorded, Fig. 6. Methyl propanoate is adsorbed intact, Fig. 6a, and also apparently desorbs intact, as there is no evidence of decomposition products remaining on the surface, Fig. 6f. On initial adsorption, the O–H stretch region clearly shows a conversion of isolated hydroxyls (negative-going peak at 3737 cm^{-1}) to a hydrogen-bonded species (Fig. 6a, intense broad peak at 3416 cm^{-1}) that progressively shifts up to 3555 cm^{-1}, Fig. 6f, as methyl propanoate desorbs (indicated by the arrow). As the isolated hydroxyls are regenerated, so the peak at 3737 cm^{-1} disappears. This is because Fig. 6 is a difference spectrum, the background spectrum has the isolated hydroxyls present, thus we are looking at changes in their numbers. The disappearance of the feature at 3737 cm^{-1} is consistent with essentially complete regeneration of the initial population of isolated hydroxyls. Temperature-programmed desorption on a similarly prepared sample showed maximum desorption at 473 K and essentially complete desorption by 573 K (see Fig. S2), consistent with Fig. 6.
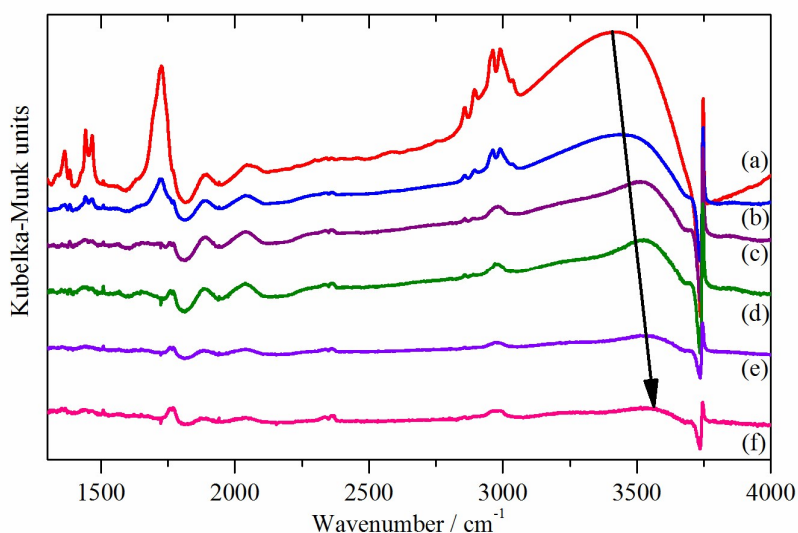

Fig. 6 Diffuse reflectance infrared difference spectra of the desorption of methyl propanoate on silica. Spectra were recorded at 303 K after heating to the stated temperature. (a) 323 K, (b) 373 K, (c) 423 K, (d) 473 K, (e) 523 K and (f) 573 K. (c) is ordinate expanded ×2, (d) and (e) ×4 and (f) ×16 all relative to (a) and (b). The arrow shows the shift to higher energy of the hydrogen-bonded O–H peak as the methyl propanoate desorbs.

13

Fig. 7 compares the infrared spectrum of solid methyl propanoate (7a) with that of the adsorbed species (7b). The carbonyl stretch is at 1727 cm^{-1} in both cases, although the band is much broader for the adsorbed species. However, there are noticeable differences in the 1300 − 1500 cm^{-1} region of the spectrum. The complexity in the spectrum of the solid material is the result of the presence of two conformers in the crystal structure. The much simpler spectrum of the adsorbed species would suggest that there is predominantly a single conformer. The periodic-DFT calculation of the solid state material was repeated but with all but one molecule removed from the unit cell. This was carried out for both conformers and the results are shown in Fig. 7 for the C_s (7c) and C_1 (7d) conformers. Neither exactly reproduces the spectrum of the adsorbed species but the C_s conformer (7c) is the better match, suggesting that this is the dominant structure.
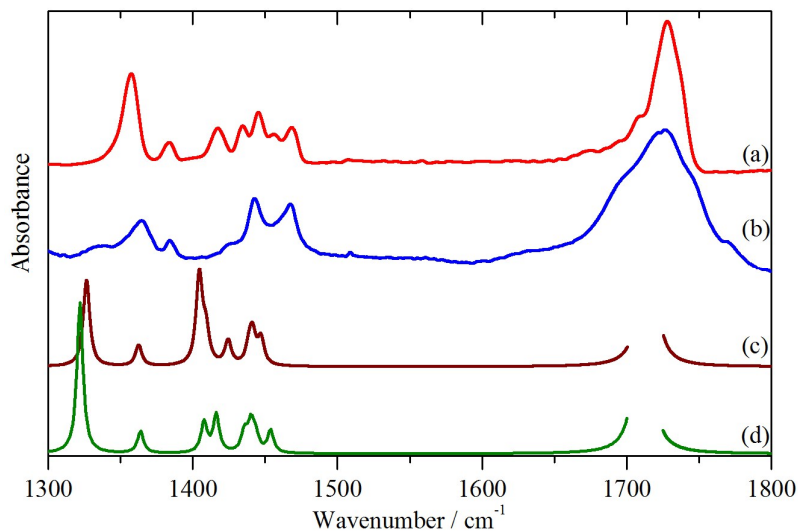
Fig. 7 Infrared spectra: (a) solid methyl propanoate at 113 K, (b) of methyl propanoate on silica after desorption at 50 °C, (c) calculated spectrum of the C_s conformer and (d) calculated spectrum of the C_1 conformer. (c) and (d) are plotted on the same scale.

The INS spectra provide a complementary view of the system. Fig. 8 shows the C–H and O–H stretch region of activated silica (8a) and after adsorption of methyl propanoate (8b). Figure 8 clearly shows the O–H stretch downshift from 3750 to 3485 cm^{-1} as a result of methyl propanoate hydrogen-bonding to the hydroxyls. This is in good agreement with the infrared results which show the peak at 3416 cm^{-1}, however, the precise location of the stretch mode in the infrared is hampered by the strong electrical anharmonicity that results from the hydrogen-bonding, this is irrelevant to INS and the location of the fundamental is easily seen.
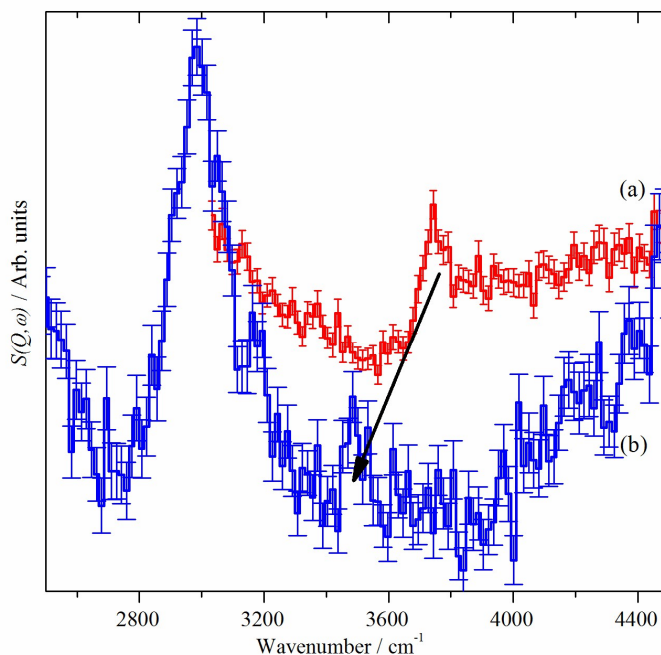
Fig. 8 INS spectra of: (a) silica after activation at 623 K and (b) methyl propanoate on silica.

As stated earlier, one of the advantages of INS spectroscopy is that common catalyst supports, carbon, alumina, silica, are essentially transparent to neutrons. The benefits of this are shown in Fig. 9 which compares the solid state spectrum of methyl propanoate (9a) with the difference spectrum, generated by subtraction of the activated silica from that of the adsorbed material (9b). Over the range $400 - 1600$ cm^{-1} the spectra are very similar, confirming molecular adsorption. This is not the case in the $0 - 400$ cm^{-1} region; in the solid state spectrum there are many more bands. This arises from four molecules with two distinct conformations in the unit cell, whereas the infrared spectra indicate (predominantly) a single conformer adsorbed on the surface.
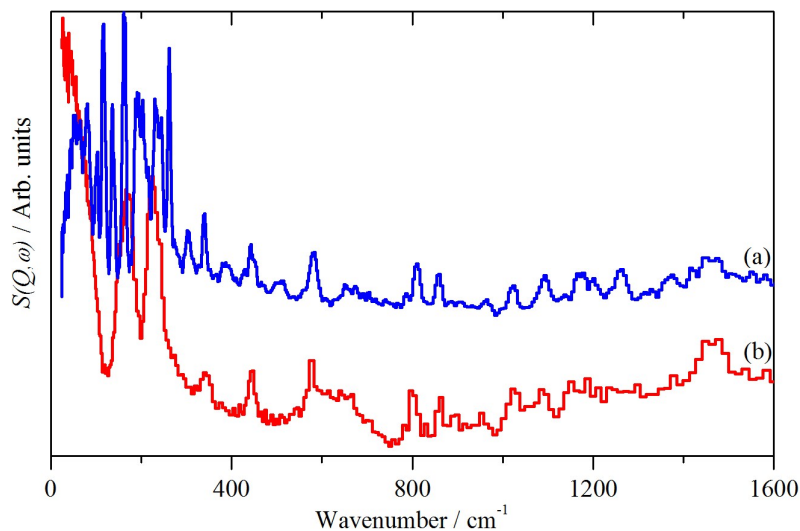
Fig. 9 INS spectra of: (a) methyl propanoate and (b) methyl propanoate on silica, after subtraction of the activated silica.

Both the infrared and the INS spectra show that methyl propanoate is hydrogen bonded to the silica hydroxyls. The 2D PES scan, Fig. 3, shows that the planar C_s conformer is the lower energy structure in the gas phase and the infrared spectrum suggests that this situation is retained on interaction with the surface. Methyl propanoate has two possible hydrogen-bond acceptor sites: the carbonyl oxygen, Fig. 10a, or the ester oxygen, Fig. 10b. To discriminate between the two possibilities the two systems were modelled with Gaussian 03 with the results shown in Table 2.
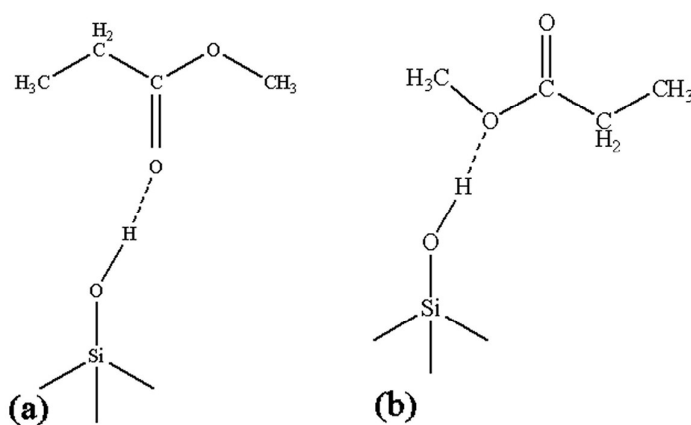

Fig. 10 Possible adsorption modes of methyl propanoate on silica: (a) *via* the carbonyl oxygen or (b) *via* the ester oxygen.

Table 2 Selected calculated vibrational transition energies for silica, free and adsorbed methyl propanoate. Values in brackets are the difference between the free and the adsorbed species.

		SiO$_2$	Methyl propanoate	Adsorbed *via* carbonyl O		Adsorbed *via* ester O		Experimental
O–H	stretch / cm^{-1}	3765		3508	(-257)	3576	(-189)	(-265)
C=O	stretch / cm^{-1}		1730	1699	(-31)	1746	(+16)	(-36)
C2–C3 + C3–O1 in-phase	stretch / cm^{-1}		836	842	(+6)	808	(-28)	(+12)

The absolute values are in modest agreement only with the data, however, the differences are likely to be much more reliable. For the species adsorbed *via* the carbonyl oxygen, the O–H stretch undergoes a large downshift, the carbonyl stretch downshifts and the skeletal stretch mode slightly upshifts, for adsorption *via* the ester oxygen, there is a somewhat smaller downshift in the O–H stretch mode, the carbonyl upshifts and the skeletal mode downshifts. The experimentally observed pattern is in almost quantitative agreement with the predictions of adsorption *via* the carbonyl oxygen.

It should be noted that the spectra of adsorbed methyl propanoate on silica resembles that of the solid in some respects, in particular, the carbonyl stretch occurs at the same transition energy ($\pm$ a few wavenumbers). Inspection of the solid state structure of methyl propanoate shows that there are weak hydrogen-bonding interactions of the type C–H····O=C present (H····O = 2.3 – 2.9 Å, $\angle$ C–H····O ~ 169°). Thus, hydrogen-bonding to the silica hydroxyls mimics to some extent the solid state, which results in the carbonyl transition energies being similar.

The possibility that there is solid methyl propanoate on the silica surface can be discounted for several reasons. The melting and boiling points of methyl propanoate are 185 and 353 K respectively; all the sample dosing was carried out at 353 K or above to minimise physisorption and the infrared spectra were recorded at 303 K, well within the liquid phase. The INS spectra in the lattice mode region, (see the 0 – 400 cm^{-1} region of Fig. 9), is distinctly different as only the internal modes of methyl propanoate are observed; those assigned (Table S3) to whole body motions are absent. The characteristic downshift and increase in intensity of the silica hydroxyls on addition of methyl propanoate is also inconsistent with the presence of solid methyl propanoate.

Figure 10(a) defines the adsorption geometry for methyl propanoate on the silica, with the silica providing Brønsted acid sites that bind the ester *via* the carbonyl group. Further work examining the adsorption and reaction of reagents on a Cs modified silica would be helpful in understanding the specific interactions associated with the industrial process. For example, INS would be insightful for determining how the addition of a Cs salt modifies the silica hydroxyl groups.

4.   Conclusions

Methyl propanoate has been characterised by a combination of vibrational spectroscopy (IR spectroscopy and INS, backed up by DFT calculations) and single crystal X-ray diffraction (Section 3, Part 1). The interaction of the ester with silica was then investigated by IR, INS and temperature-programmed desorption. The following conclusions can be drawn.

- The structure of methyl propanoate as determined by X-ray diffraction is triclinic, space group $P\bar{1}$. DFT calculations show the planar C_s conformation to be the lower energy structure. Experimental IR and INS spectra of methyl propanoate are combined with associated DFT calculations to provide a complete vibrational assignment.

- Adsorption experiments of methyl propanoate on silica employing temperature-programmed IR spectroscopy and temperature-programmed desorption show the methyl propanoate to be molecularly adsorbed on the silica. Both IR and INS spectra of the adsorption complex show methyl propanoate to be hydrogen-bonded to silica hydroxyls, with adsorption occurring *via* the carbonyl group of methyl propanoate.

- Silica hydroxyl groups constitute weak Brønstead acid sites that bind methyl propanoate.

References

1.   K. Nagai, *Appl. Catal. A: Gen*., 2001, **221**, 367.

2.   A. Tullo, *Chem. Engineering News*, 2009, **87(42)**, 22-23.

3.   J. Tai and R. J. Davis, *Catal. Today*, 2007, **123**, 42.

4.   http://www.luciteinternational.com/ (accessed 20/02/2016).

5.   K. AlGhamdi, J. S. J. Hargreaves and S. D. Jackson in *Metal Oxide Catalysis*, Eds. S.D. Jackson and J.S.J. Hargreaves, Wiley-VCH, Weinheim, 2009, p.819-843.

6.   S.D. Jackson, G.J. Kelly and D. Lennon, *React. Kinet. Catal. Lett.*, 2000, **70**, 207.

7.   S.D. Jackson, D.W. Johnson, J.D. Scott, G.J. Kelly, B.P. Williams (Imperial Chemical Industries Plc, UK), Patent PCT Int. Appl. WO9952628-A1 (1999).

8.   J. Cosier and A. M. Glazer, *J. Appl. Cryst.*, 1986, **105**, 107.

9.   Nonius (2001). COLLECT. Nonius BV, Delft, The Netherlands.

10.   Z. Otwinowski and W. Minor, *Methods in Enzymology*, 276, Eds. C. W. Carter Jr and R. M. Sweet, pp. 307–326. Academic Press, New York, 1997.

11.   L. Palatinus and G. Chapuis, *J. Appl. Cryst.*, 2007, **40**, 786–790.

12.   P. W. Betteridge, J. R. Carruthers, R. I. Cooper, K. Prout and D. J. Watkin, *J. Appl. Cryst.*, 2003, **36**, 1487.

13.   D. J. Watkin, C. K. Prout and L. J. Pearce,. CAMERON, Chemical Crystallography Laboratory, Oxford, UK, 1996.

14.   S. J. Clark, M. D. Segall, C. J. Pickard, P. J. Hasnip, M. J. Probert, K. Refson and M. C. Payne, *Z. Krist.*, 2005, **220**, 567.

15.   K. Refson, P. R. Tulip, S. J. Clark, *Phys. Rev. B*, 2006, **73**, 155114.

16.   Gaussian 03, Revision B.05, M. J. Frisch, G. W. Trucks, H. B. Schlegel, G. E. Scuseria, M. A. Robb, J. R. Cheeseman, J. A. Montgomery, Jr., T. Vreven, K. N. Kudin, J. C. Burant, J. M. Millam, S. S. Iyengar, J. Tomasi, V. Barone, B. Mennucci, M. Cossi, G. Scalmani, N. Rega, G. A. Petersson, H. Nakatsuji, M. Hada, M. Ehara, K. Toyota, R. Fukuda, J. Hasegawa, M. Ishida, T. Nakajima, Y. Honda, O. Kitao, H. Nakai, M. Klene, X. Li, J. E. Knox, H. P. Hratchian, J. B. Cross, V. Bakken, C. Adamo, J. Jaramillo, R. Gomperts, R. E. Stratmann, O. Yazyev, A. J. Austin, R. Cammi, C. Pomelli, J. W. Ochterski, P. Y. Ayala, K. Morokuma, G. A. Voth, P. Salvador, J. J. Dannenberg, V. G. Zakrzewski, S. Dapprich, A. D. Daniels, M. C. Strain, O. Farkas, D. K. Malick, A. D. Rabuck, K. Raghavachari, J. B. Foresman, J. V. Ortiz, Q. Cui, A. G. Baboul, S. Clifford, J. Cioslowski, B. B. Stefanov, G. Liu, A. Liashenko, P. Piskorz, I. Komaromi, R. L. Martin, D. J. Fox, T. Keith, M. A. Al-Laham, C. Y. Peng, A. Nanayakkara, M. Challacombe, P. M. W. Gill, B. Johnson, W. Chen, M. W. Wong, C. Gonzalez, and J. A. Pople, Gaussian, Inc., Wallingford CT, 2004.

17.   A. J. Ramirez-Cuesta, Comput. Phys. Commun., 2004, **157**, 226.

18.   T. Lear, R. Marshall, J.A. Lopez-Sanchez, S.D. Jackson, T. M. Klapötke, G. Rupprechter, M. Bäumer, H-J. Freund and D. Lennon, *J. Chem. Phys.,* 2005, **123**, 174706.

19.   P.C.H. Mitchell, S.F. Parker, A.J. Ramirez-Cuesta and J. Tomkinson, *Vibrational spectroscopy with neutrons, with applications in chemistry, biology, materials science and catalysis*, World Scientific, Singapore, 2005.

20.   S.F. Parker, D. Lennon and P.W. Albers, *Applied Spectroscopy,* 2011, **65**, 1325-1341.

21.   D. Colognesi, M. Celli, F. Cilloco, R.J. Newport, S.F. Parker, V. Rossi-Albertini, F. Sacchetti, J. Tomkinson and M. Zoppi, *Appl. Phys. A* 74 [Suppl.] (2002) S64–S66.

22.   http://www.isis.stfc.ac.uk/ (accessed 19th April 2016)

23.   I.P. Silverwood , N.G. Hamilton , A. McFarlane , R.M. Ormerod, T. Guidi, J. Bones, M.P. Dudman, C.M. Goodway, M. Kibble, S.F. Parker and D. Lennon, *Rev. Sci. Inst.*, 2011, **82**, 034101.

Table 1 Vibrational transition energies of methyl propanoate in the solid state and adsorbed on silica.

Mode	Solid state / cm^{-1}	Adsorbed on SiO_2 / cm^{-1}
C=O stretch	1728	1726
C4 Methyl asym def	1469, 1456	1468
C4 Methyl sym deformation	1445, 1432	1442
Methylene scissors	1417	1427
C1 Methyl sym deformation	1384	1384
Methylene wag	1356	1364
C1 methyl rock	1092	1090
C1 methyl rock	1024	1029
C1–C2 + O1–C4 out-of-phase stretch	962	953
C2–C3 + C3–O1 in-phase stretch	858	859
Methylene rock	809	802
C=O out-of-plane bend	581	577
C2–C3–O1 in-plane bend	443	445
C1–C2–C3 + C3–C1–C4 out-of-phase, in-plane bend	339	343
C1 methyl torsion	263, 244, 231	225
C1 methyl torsion and C3–O1 torsion	204, 192, 163	170